Direct conversion of carlactonoic acid to orobanchol by cytochrome P450 CYP722C in strigolactone biosynthesis

Wakabayashi, Takatoshi ; Hamana, Misaki ; Mori, Ayami ; Akiyama, Ryota ; Ueno, Kotomi ; Osakabe, Keishi ; Osakabe, Yuriko ; Suzuki, Hideyuki …

(Citation)
Science Advances,5(12):eaax9067-eaax9067

(Issue Date)
2019-12

(Resource Type)
journal article

(Version)
Version of Record

(URL)
https://hdl.handle.net/20.500.14094/90006672

PLANT SCIENCES

Direct conversion of carlactonoic acid to orobanchol by cytochrome P450 CYP722C in strigolactone biosynthesis

Takatoshi Wakabayashi[1], Misaki Hamana[1], Ayami Mori[1], Ryota Akiyama[1], Kotomi Ueno[1]*, Keishi Osakabe[2], Yuriko Osakabe[2], Hideyuki Suzuki[3], Hirosato Takikawa[1†], Masaharu Mizutani[1], Yukihiro Sugimoto[1‡]

Strigolactones (SLs) are carotenoid-derived phytohormones and rhizosphere signaling molecules for arbuscular mycorrhizal fungi and root parasitic weeds. Why and how plants produce diverse SLs are unknown. Here, cytochrome P450 CYP722C is identified as a key enzyme that catalyzes the reaction of BC-ring closure leading to orobanchol, the most prevalent canonical SL. The direct conversion of carlactonoic acid to orobanchol without passing through 4-deoxyorobanchol is catalyzed by the recombinant enzyme. By knocking out the gene in tomato plants, orobanchol was undetectable in the root exudates, whereas the architecture of the knockout and wild-type plants was comparable. These findings add to our understanding of the function of the diverse SLs in plants and suggest the potential of these compounds to generate crops with greater resistance to infection by noxious root parasitic weeds.

INTRODUCTION

Strigolactones (SLs) are a class of phytohormones that regulate many aspects of plant architecture and development. In addition, SLs are important signaling molecules in the rhizosphere, inducing hyphal branching of arbuscular mycorrhizal fungi (AMF) and stimulating the seed germination of noxious root parasitic weeds (*1*–*5*). In plants, up-regulation of the synthesis of SLs may be an adaptive defense against phosphorus (Pi) starvation through minimization of shoot branching and maximization of symbiotic interaction with AMF, providing Pi (*2*, *6*). SLs secreted into the soil could also serve as germination signals for seeds of root parasitic weeds. Thus, crops producing a limited amount of SLs can avoid adverse effects caused by the parasites. Furthermore, the biomass and production of seeds and fruits are linked directly to plant architecture. Therefore, to use SL for agriculture, elucidation of SL biosynthesis is required.

SLs can be classified into canonical and noncanonical SLs. Canonical SLs consist of a tricyclic lactone ring system (ABC-ring) connected to a methyl butenolide (D-ring) via an enol ether bridge, and noncanonical SLs have an unclosed BC-ring (Fig. 1A). Canonical SLs are either orobanchol or strigol types, which have 8b*R* and 8b*S* stereochemistry in the C-ring, respectively. To date, 23 canonical SLs and several noncanonical SLs have been identified in root exudates of a variety of plant species (*7*–*11*). The chemical structure of most canonical SLs consists of derivatives of 4-deoxyorobanchol (4DO) and 5-deoxystrigol (5DS), which have the simplest structures of orobanchol- and strigol-type SLs, respectively. SL biosynthesis begins with DWARF 27 (D27) catalysis of isomerization of the C9-C10 double bond in all-*trans*-β-carotene, followed by carotenoid cleavage dioxygenase 7 (CCD7) and CCD8 catalysis of sequential carotenoid cleavage reactions (*12*, *13*) to form a biosynthetic intermediate, carlactone (CL). Cytochrome P450 (CYP) monooxygenase CYP711A encoded by more axillary growth 1 (*MAX1*), first identified in *Arabidopsis*, catalyzes oxidation of CL at C-19 to produce carlactonoic acid (CLA) (Fig. 1A) (*14*). To date, in all the plants examined, CYP711As convert CL to CLA, suggesting that CLA is a common precursor for SL biosynthesis (*15*, *16*). For canonical SLs, the biosynthetic pathway downstream of CLA featuring a BC-ring closure reaction catalyzed by MAX1 homologs has been reported in rice and *Selaginella moellendorffii* (*15*, *17*). The ring closure reaction converting CL to 4DO via CLA is catalyzed by rice CYP711A2/Os900 and *S. moellendorffii* CYP711A17v1 and CYP711A17v3, and a hydroxy group is introduced by rice CYP711A3/Os1400 at C-4 of 4DO to generate orobanchol (Fig. 1A) (*15*, *17*). However, other previously examined MAX1 homologs did not catalyze the conversion of CLA to canonical SL via the ring closure reaction (*15*–*17*).

Despite intensive previous research, the downstream pathway of CLA is still not well understood, and the functional hormone has not been identified. The identification of an enzyme that catalyzes the conversion of CLA to canonical SL will help elucidate whether the genuine hormone is a canonical or noncanonical SL (*11*).

RESULTS AND DISCUSSION

Previously, in cowpea (*Vigna unguiculata*) (*18*) and several orobanchol-producing plants (*19*), we demonstrated that exogenously administered *rac*-CLA was bioconverted to orobanchol and orobanchyl acetate without passing through 4DO. In cowpea, this bioconversion was inhibited by uniconazole-P, a CYP inhibitor; in contrast, the conversion was not inhibited by prohexadione, a 2-oxoglutarate–dependent dioxygenase (DOX) inhibitor (Fig. 1B). This result was in good agreement with those previously reported for inhibitor treatments in tomato (*Solanum lycopersicum*), another orobanchol-producing plant, in which CYP inhibition blocked the conversion of CLA to orobanchol more strongly than DOX inhibition (*16*). Therefore, CYP involvement in direct conversion of CLA to orobanchol was predicted. First, the function of cowpea VuMAX1 was characterized. In cowpea, two MAX1 homologous genes, namely, *Vigun09g224400* and *Vigun08g039400*, are recorded in the Phytozome database [*V. unguiculata* v1.0; National Science Foundation (NSF); University

[1]Graduate School of Agricultural Science, Kobe University, 1-1 Rokkodai, Nada, Kobe 657-8501, Japan. [2]Graduate School of Technology, Industrial and Social Sciences, Tokushima University, Tokushima 770-8503, Japan. [3]Kazusa DNA Research Institute, Kazusa-kamatari 2-6-7, Kisarazu, Chiba 292-0818, Japan.
*Present address: Faculty of Agriculture, Tottori University, Koyama, Tottori, 680-8553, Japan.
†Present address: Graduate School of Agricultural and Life Sciences, The University of Tokyo, 1-1-1 Yayoi, Bunkyo-ku, Tokyo 113-8657, Japan.
‡Corresponding author. Email: yukihiro@kobe-u.ac.jp

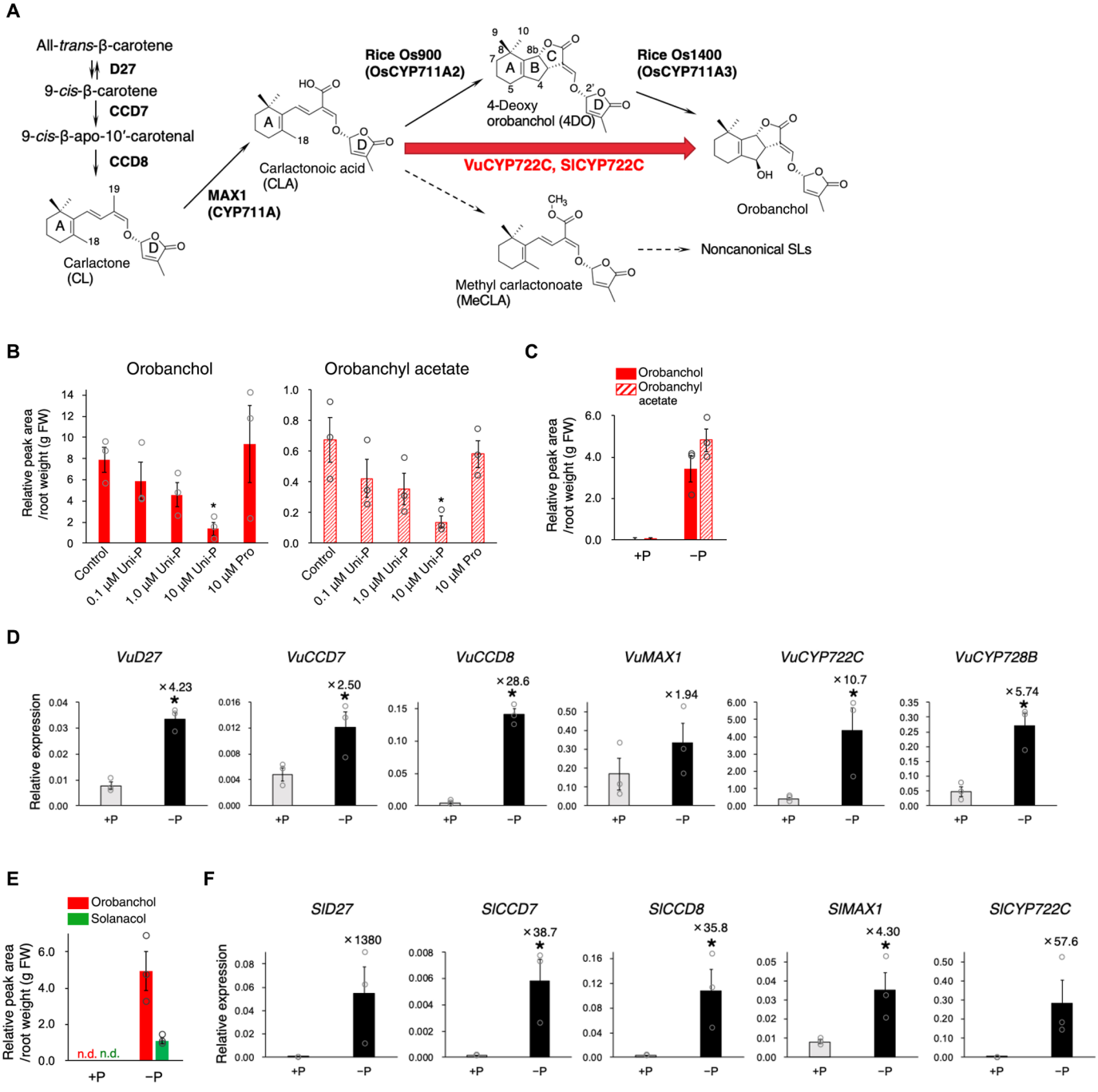

Fig. 1. The orobanchol pathway catalyzed by CYP722C and the expressions of SL biosynthesis genes in roots. (**A**) Proposed biosynthesis pathway of SLs. The enzyme catalyzing the reaction indicated by the red bold arrow was identified in this study. Dashed arrows indicate putative pathway. (**B**) Effect of uniconazole-P (Uni-P) and prohexadione (Pro) on bioconversion of CLA to orobanchol and orobanchyl acetate in cowpea plants. After administering *rac*-CLA for 24 hours in the presence of the inhibitors, root exudates of cowpea were analyzed with LC-MS/MS. Each peak area was calculated relative to an internal standard (2′-*epi*-strigol). Error bars represent means ± SE ($n = 3$ biologically independent plants). FW, fresh weight. Asterisk indicates significant difference between control and inhibitor treatment (*$P < 0.05$, Student's *t* test). (**C** to **F**) Quantification of SLs in root exudate of cowpea and tomato cultivated under Pi-rich (+P) and Pi-deficient (−P) conditions (C and E) and expression of SL biosynthesis genes in their roots (D and F). Each peak area in (C) and (E) was calculated relative to an internal standard (2′-*epi*-strigol). The number above the bar in (D) and (F) indicates fold change of expression level in −P with respect to +P. Expression level was normalized to endogenous cowpea actin or tomato ubiquitin mRNA levels. Error bars represent means ± SE ($n = 3$ biologically independent plants). n.d., not detected. Asterisk indicates significant difference between +P and −P (*$P < 0.05$, Student's *t* test).

of California, Riverside (UCR); United States Agency for International Development (USAID), and Department of Energy Joint Genome Institute (DOE-JGI); http://phytozome.jgi.doe.gov/]; however, because gene expression of *Vigun08g039400* was below the detection limit via quantitative real-time reverse transcription polymerase chain reaction (qRT-PCR), the *Vigun09g224400* transcript with a higher expression level was selected for further functional analysis as VuMAX1. As reported for MAX1 homologs (*15*, *16*), recombinant VuMAX1 catalyzed the conversion of CL to CLA; however, recombinant VuMAX1 did not catalyze the conversion of CLA to 4DO or orobanchol (Fig. 2). This result suggested that a CYP, which differs from CYP711As, is responsible for the conversion of CLA to orobanchol. Notably, Zhang *et al.* (*17*) suggested that a gene other than *CYP711A3*/*Os1400* is involved in orobanchol formation in rice because the cultivar Bara, which is deficient in *CYP711A3*/*Os1400*, retains the ability to produce orobanchol. Thus, our goal was to identify a previously unknown CYP that catalyzes the direct orobanchol formation from CLA.

Production of SLs by cowpea markedly differed under different hydroponic conditions (fig. S1). Previously, the observation of increased SL levels in root exudates in Pi-deficient cultures has been reported (*6*). We administered the synthetic SL, *rac*-GR24, to Pi-deficient cultures, anticipating that SL levels decreased because of the feedback regulation of SL biosynthesis genes (*20*). Contrary to our expectation, SL levels increased under this condition (fig. S1B). The mechanism of the increased production of SL is unknown, but it was considered that a substantial increase in SL levels would reflect the up-regulation of SL biosynthesis genes. Then, transcriptome analysis with de novo RNA sequencing (RNA-seq) of the roots grown in the established hydroponic conditions was conducted, focusing on putative SL biosynthesis genes. Their expression should be correlated with SL production. With these RNA-seq datasets, detailed coexpression gene network analysis was performed using the Confeito algorithm (*21*), which generated a module of cowpea *CCD8* (*VuCCD8*) transcripts (data S1). This module contained *VuCCD7*, which is another SL biosynthesis transcript, SL receptor *VuD14*, and several transcripts encoding carotenoid biosynthesis. The pathway from carotenoid to SL was indicated by coexpression of *VuCCD8* with carotenoid biosynthesis genes, which are located upstream of SL biosynthesis genes. From the *VuCCD8* module, which included seven transcripts encoding CYPs (table S1), we selected uncharacterized transcripts *CYP722C* and *CYP728B* as candidates for a orobanchol synthase gene. Up-regulation of *VuCYP722C* and *VuCYP728B* genes, as well as *VuD27*, *VuCCD7*, *VuCCD8*, and *VuMAX1* genes, which are homologous to known SL biosynthetic genes, was demonstrated by qRT-PCR analysis in cowpea roots cultivated under Pi-deficient conditions with an increase in SL levels in the root exudates (Fig. 1, C and D, and fig. S2A). This result indicated the coexpression of *VuCYP722C* and *VuCYP728B* genes with SL biosynthetic genes, suggesting that these two genes are involved in SL biosynthesis in cowpea.

VuCYP722C and *VuCYP728B* complementary DNAs (cDNAs) were cloned and heterologously expressed in an insect cell expression system. Orobanchol was not produced from incubation of the recombinant VuCYP728B with *rac*-CLA (fig. S3A). In contrast, compounds corresponding to authentic standards of *rac*-orobanchol and its diastereomer *rac*-2′-*epi*-orobanchol were produced by incubating VuCYP722C with *rac*-CLA (Fig. 3A). The natural stereoisomer of CLA was converted to orobanchol and *ent*-2′-*epi*-orobanchol by the enzyme (fig. S4B). The conversion of *rac*-4DO to orobanchol was not catalyzed by the recombinant VuCYP722C (fig. S4C), consistent with our previous result that exogenously administered 4DO in cowpea hydroponic culture was not converted to orobanchol (*18*).

In addition, a compound eluted at a retention time of 8.25 min was detected at a multiple reaction monitoring (MRM) transition of mass/charge ratio (*m*/*z*) 347 > 113 in negative-ion mode in liquid chromatography–tandem mass spectrometry (LC-MS/MS) analysis

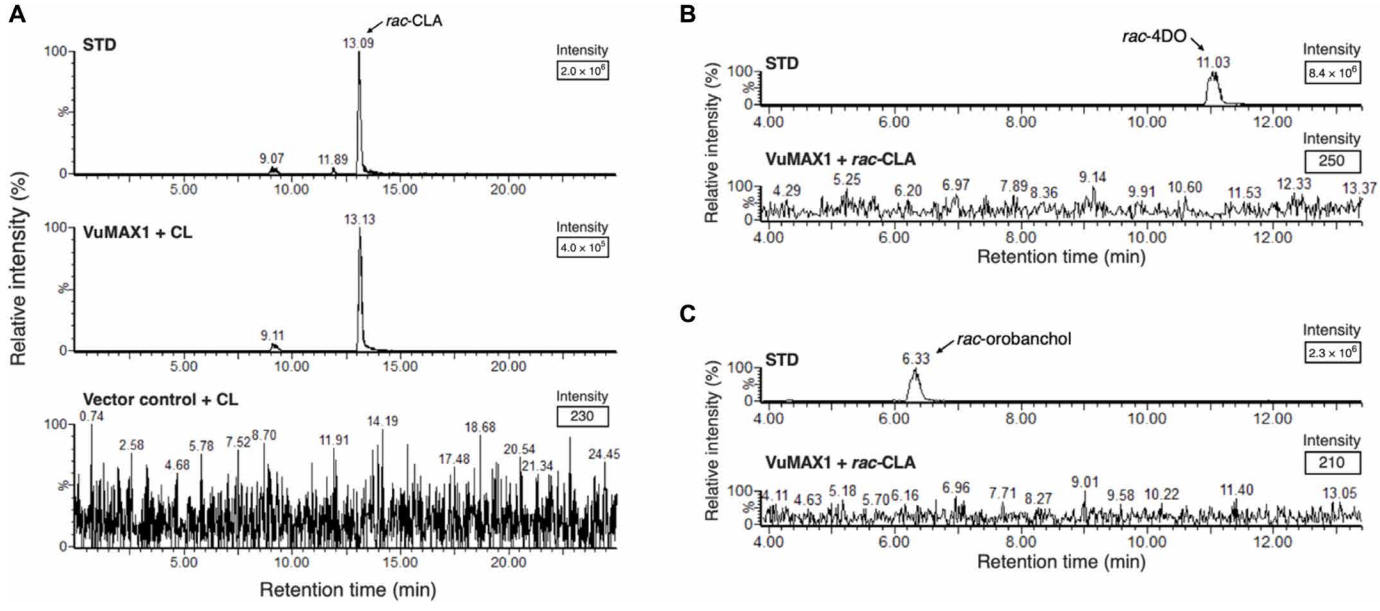

Fig. 2. In vitro enzyme assay of recombinant VuMAX1. Multiple reaction monitoring (MRM) chromatograms of reaction mixture of recombinant VuMAX1 with CL (**A**) and *rac*-CLA (**B** and **C**) as substrates using LC method I, showing MRM transitions for CLA (A), 4DO (B), and orobanchol (C). The ion intensities are given in the top right square of each chromatogram.

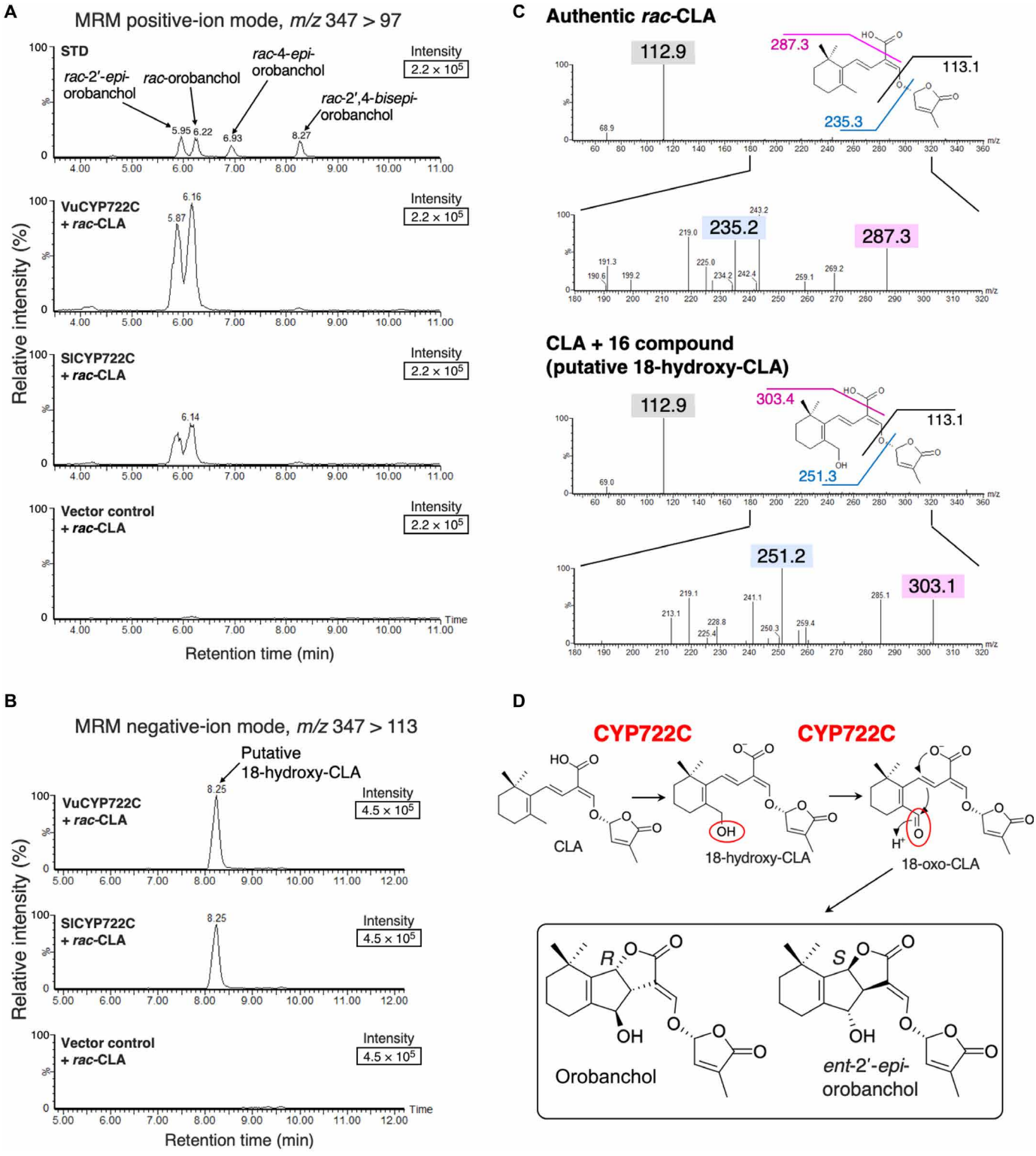

Fig. 3. In vitro enzyme assay for production of orobanchol by recombinant CYP722C enzyme. (**A** and **B**) MRM chromatograms of reaction mixture of recombinant CYP722C with *rac*-CLA as the substrate. LC method I was used to separate SLs. (A) MRM transition of *m/z* 347 > 97 in positive electrospray ionization (ESI) mode was selected for orobanchol. (B) The CLA + 16 compound detected at an MRM transition of *m/z* 347 > 113 in negative ESI mode. The top right square of each chromatogram shows the ion intensities. These data represent results from more than three independent experiments. (**C**) Product ion spectra derived from the precursor ion $[M - H]^-$ of *m/z* 331.2 of CLA (top) and $[M - H]^-$ of *m/z* 347.2 of putative 18-hydroxy-CLA (bottom). (**D**) Proposed mechanism of orobanchol production with BC-ring formation catalyzed by CYP722C.

as a product in the reaction mixture of the recombinant VuCYP722C with *rac*-CLA (Fig. 3B). This compound may be a biosynthetic intermediate to orobanchol, most likely 18-hydroxy-CLA. The ion $[M - H]^-$ at *m/z* 347 corresponded to CLA + 16 Da. The MS/MS fragment pattern of the compound shared common characteristic fragment ions *m/z* 113 and 69 with CLA and displayed fragment ions *m/z* 303 and 251 larger than those of CLA by 16 Da (Fig. 3C). This fragment pattern was consistent with that of previously reported putative 18-hydroxy-CLA (*15*). On the basis of these results, with reference to the previously proposed model (*3*), we propose the following molecular mechanism of the reaction catalyzed by VuCYP722C: The two-step oxidation at the C-18 position in CLA generates 18-oxo-CLA via 18-hydroxy-CLA, and the BC-ring closure reaction without stereoselective control of 18-oxo-CLA proceeds to yield orobanchol stereoisomers (Fig. 3D).

The function of CYP722C was also confirmed in tomato, whose direct biosynthesis of orobanchol from CLA has also been suggested (*16*). The expression of *SlCYP722C* was up-regulated in Pi-deficient conditions with incremental expression of known SL biosynthetic genes and SL production (Fig. 1, E and F, and fig. S2, B to D). Recombinant SlCYP722C catalyzed the same reaction as VuCYP722C (Fig. 3, A and B, and fig. S3C). *Ent*-2′-*epi*-orobanchol has not been identified in cowpea and tomato. Thus, these orobanchol-producing plants may be equipped with a mechanism for controlling the configuration of the C-ring structure that acts in coordination with CYP722C.

To characterize the function of CYP722C in planta, we generated *SlCYP722C*-knockout (*SlCYP722C*-KO) tomato plants by CRISPR-Cas9–mediated genome editing. Indels in the gene that resulted in biallelic frameshift mutations were identified in the T1 transgenic plants (Fig. 4, A and B). We used T2 progeny lines harboring the same biallelic mutation as the T1 lines for further analyses. In root exudates of *SlCYP722C*-KO plants, orobanchol and solanacol, a possible metabolite of orobanchol, were not detected, but CLA was detected, which was not observed in root exudates of wild-type (WT) plants (Fig. 5, A to D). In addition, CLA accumulation was confirmed in the root extracts of *SlCYP722C*-KO plants (fig. S4A). These results are consistent with the proposed molecular mechanism (Fig. 3D) by which CYP722C catalyzes orobanchol synthesis from CLA with the BC-ring closure reaction. The expression of SL biosynthesis genes has been reported to be up-regulated in tomato *Slmax1* mutants and *SlCCD8*–RNA interference lines (*16*); however, the expression of the four SL biosynthesis genes that act upstream of *SlCYP722C* was not significantly changed in roots of *SlCYP722C*-KO plants compared with those of WT (Fig. 6A). Therefore, in *SlCYP722C*-KO plants, synthesis of CLA from β-carotene was likely normal; however, CLA accumulated owing to the loss of function of orobanchol synthase. Thus, we conclude that CYP722C is a novel orobanchol synthase.

The *CYP722* family is found in monocot and dicot genomes but has not been identified in land plants outside the angiosperms (*22*). The MAX1 homologs of *S. moellendorffii*, a common ancestor of angiosperms, participate in the BC-ring closure of CLA to generate canonical SL, whereas most MAX1 homologs in monocots and dicots have lost this function (*15*), suggesting that the acquisition of new functionality by CYP722 family enzymes in the monocot-dicot divergence during the evolution of angiosperms probably results in different biosynthetic mechanisms for canonical SLs and the loss of some MAX1 functions. Functional analysis of CYP722 family enzymes in various plants will enable us to elucidate the transition of the biosynthetic mechanism of canonical SLs and its origin.

SlCYP722C-KO plants did not show the prominent phenotypes of the SL-deficient mutant *Slccd8*, such as increased shoot branching

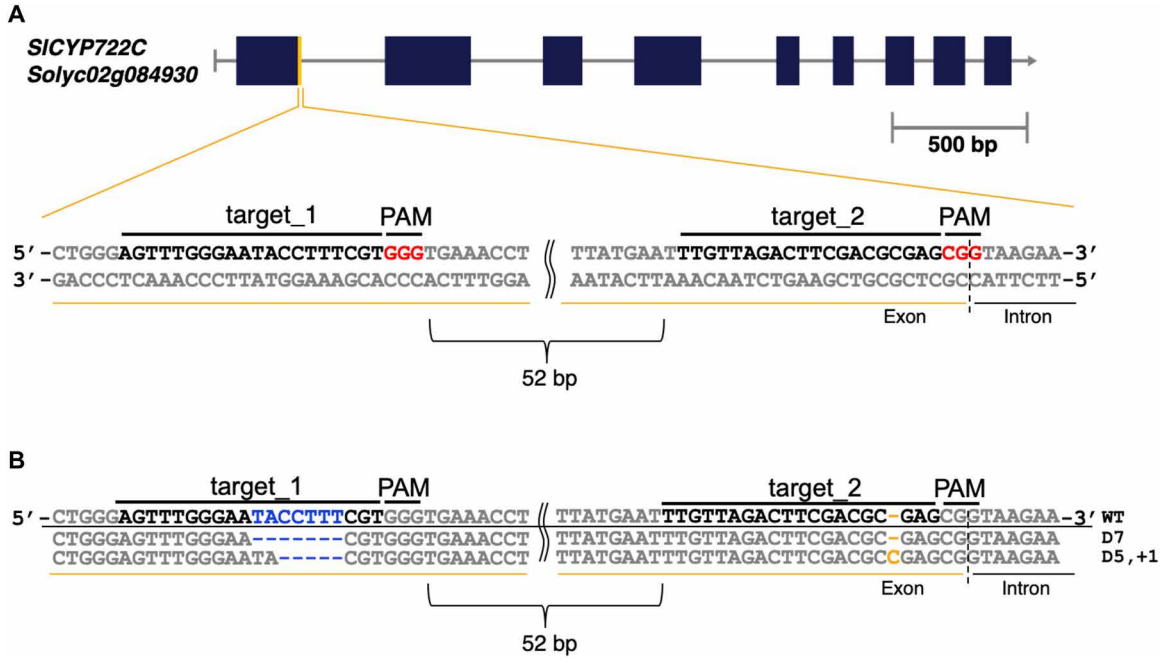

Fig. 4. Targeted mutation in the tomato *SlCYP722C* locus mediated by the CRISPR-Cas9 system. (**A**) The structure of *SlCYP722C* and the CRISPR-Cas9 target sites (gRNA target_1 and target_2). Each target region is shown in bold letters followed by red protospacer adjacent motif (PAM). (**B**) Genotyping DNA sequences surrounding *SlCYP722C* in T1 transgenic tomato plants compared with the WT sequence shown on the first line. The number of deleted (D) and inserted (+) nucleotides is shown on the right. The T2 lines with the same biallelic mutation as the T1 lines shown in here were used for further analyses.

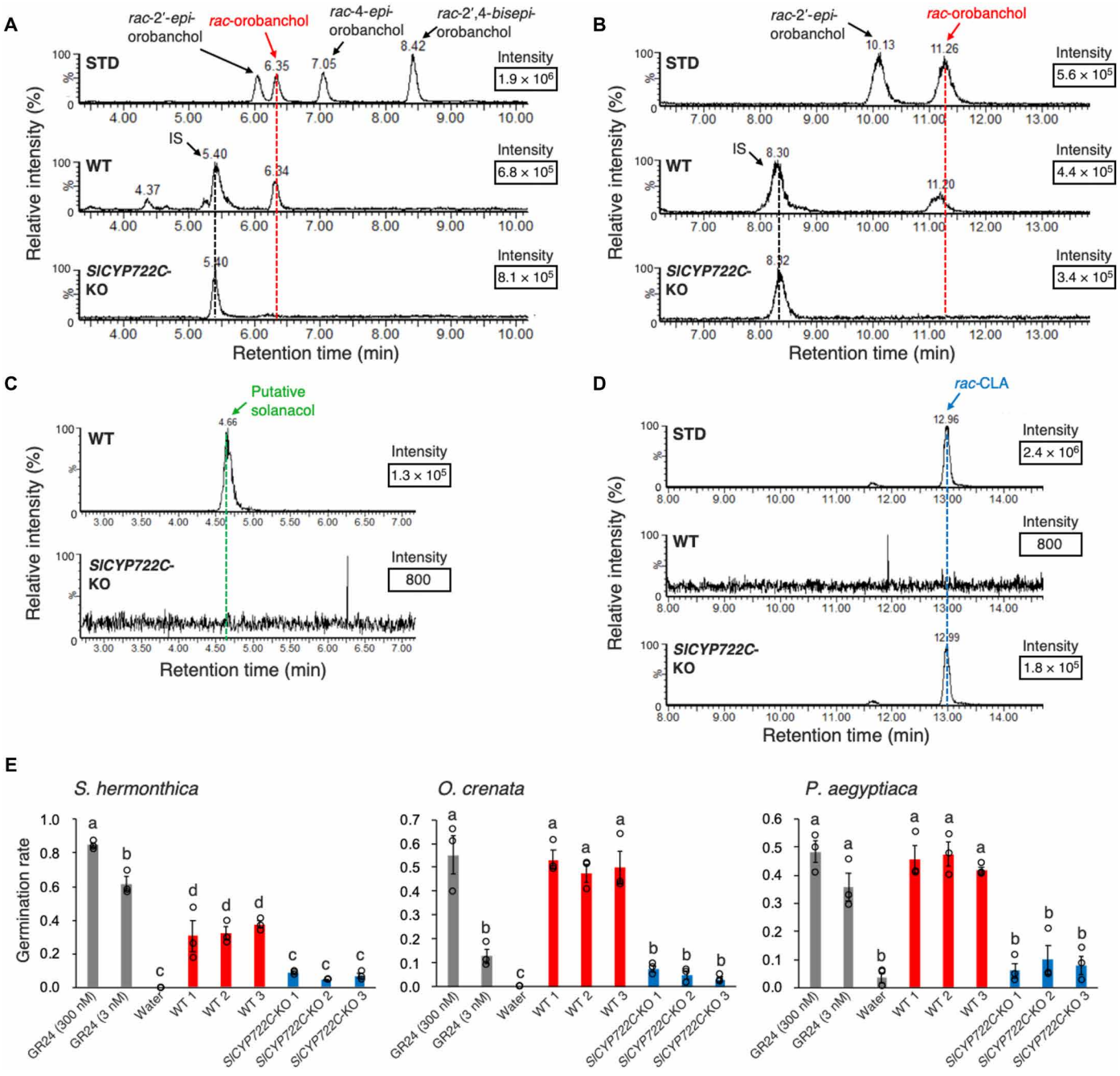

Fig. 5. Analysis of root exudates in *SlCYP722C*-KO plants. (**A** to **D**) MRM chromatograms of the root exudates of WT and KO plants cultivated under Pi-deficient conditions. The ion intensities are shown in the top right square of each chromatogram. IS, internal standard (2′-*epi*-strigol). Solanacol was putatively identified because an authentic standard was not available. LC method I was used to separate SLs (A, C, and D), and LC method II was applied for greater peak resolution of orobanchol isomers (B). These data represent results from more than three independent experiments. (**E**) Effect of root exudates of *SlCYP722C*-KO plants on induction of seed germination of root parasitic weeds. A synthetic SL, GR24, and water were used as positive and negative controls, respectively. Error bars represent means ± SE ($n = 3$ biologically independent experiments). Different letters indicate significant differences in the germination rate ($P < 0.05$, Tukey-Kramer test).

and reduced stem length (Fig. 6, B to D) (*23*). Methyl carlactonoate (MeCLA) is known to potentially function as an active hormone that inhibits shoot branching in *Arabidopsis* (*14*); however, MeCLA was undetectable in root exudates and root and shoot extracts in *SlCYP722C*-KO plants, and it was unclear whether MeCLA contributes to the regulation of plant architecture in *SlCYP722C*-KO plants (fig. S4B). Combined with the result of unaltered gene expression, deficiency of the *SlCYP722C* seems largely inconsequential for the overall biosynthesis of SL with activity as a phytohormone that regulates plant architecture. In contrast, root exudates of *SlCYP722C*-KO plants reduced the induction of germination of seeds of root parasitic weeds, *Striga hermonthica*, *Orobanche crenata*, and *Phelipanche aegyptiaca*,

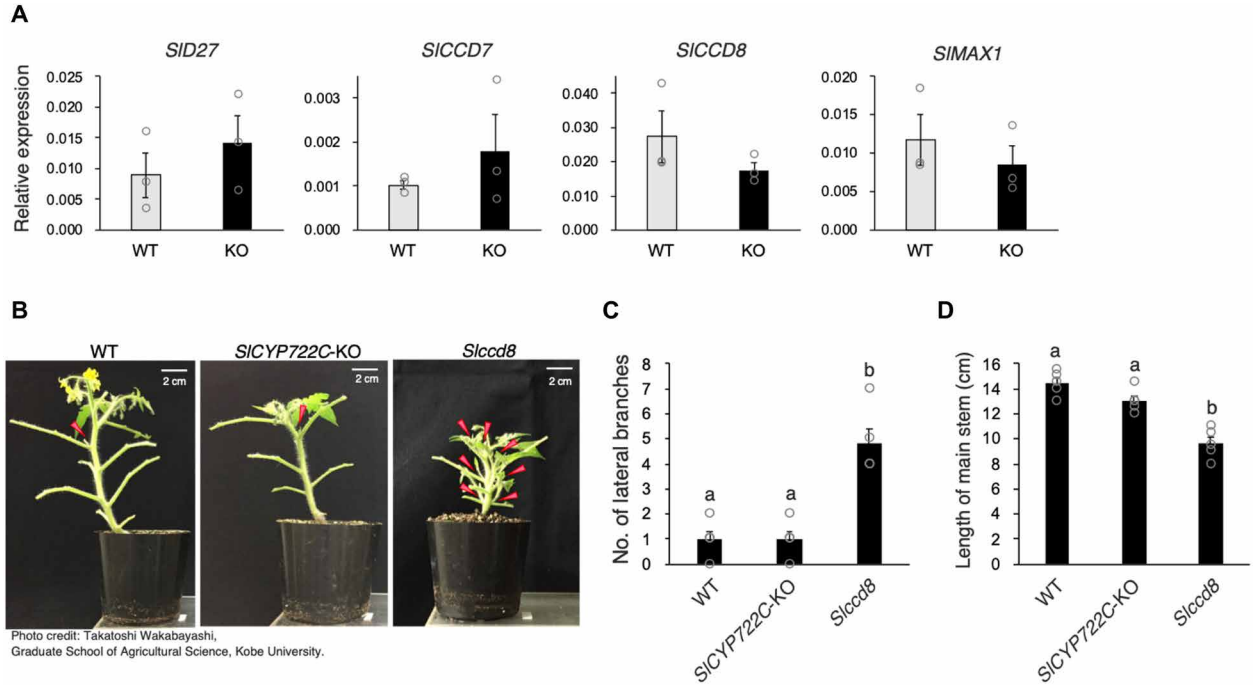

Fig. 6. Effect of targeted mutation in *SlCYP722C*. (**A**) Gene expression of SL biosynthesis genes that act upstream of *SlCYP722C* in *SlCYP722C*-KO plants. WT and KO plants did not significantly differ. Error bars represent means ± SE ($n = 3$ biologically independent plants). (**B** to **D**) Comparisons of shoot branching (C) and stem length (D) between WT, *SlCYP722C*-KO, and SL-deficient mutant *Slccd8* (line 2757) (*23*). Red arrows indicate outgrowing axillary buds (>2 mm). Branches (>2 mm) were counted, and main stem lengths were measured for 50 days. Error bars represent means ± SE ($n = 5$ biologically independent plants). Different letters indicate significant differences ($P < 0.05$, Tukey-Kramer test).

compared to WT (Fig. 5E). Together, these results imply that canonical SLs, such as orobanchol and solanacol, are potent signaling molecules in the rhizosphere. A more detailed analysis of *SlCYP722C*-KO plants will allow characterization of the active compound as a true phytohormone.

Moreover, *CYP722C*-KO plants have the potential to combat noxious root parasitic weeds. *SlCYP722C*-KO plants reduce the germination of *P. aegyptiaca*, a serious constraint on tomato production (*23*, *24*), without changing the plant architecture, and they release CLA from the roots. The activity of CLA against the hyphal branching of AMF was comparable with that of natural canonical SLs such as strigol and sorgomol (*25*), suggesting that CLA can be used as a signaling molecule to facilitate symbiotic interactions with AMF. In addition, the T1 *SlCYP722C*-KO plant produced fruits and seeds normally, and T2 progeny was generated, suggesting that no serious yield loss occurs even in crops lacking the *CYP722C* gene. It is our further goal to evaluate the applicability of *CYP722C* gene deficiency to agriculture by using more practical varieties of tomato and other crops.

MATERIALS AND METHODS

Chemicals

Authentic samples of CL, 5DS isomers, orobanchol isomers, and *rac*-MeCLA were prepared as previously described (*18*, *26*). Synthesis of *rac*-CLA is described in the Supplementary Text.

Plant hydroponic culture and SL extraction from culture media and plants

Seedlings of cowpea (*V. unguiculata* cv. B301) were grown hydroponically with half-strength Hoagland nutrient solution in a growth chamber at 23°C and a 16-hour light/8-hour dark photoperiod for 2 weeks as described previously (*18*). The seedlings were transferred to half-strength Hoagland nutrient solution (Pi rich) or tap water (Pi deficient). After 3 days, the culture media were replaced with fresh media, and plants were grown for 24 hours. Bioconversion experiments of SL precursors with inhibitors were performed as described previously (*18*).

Seeds of tomato (*S. lycopersicum* cv. Micro-Tom) were sown on Murashige-Skoog agar plates and cultivated at 23°C in the dark for 5 days and then cultivated at 23°C with a 16-hour light/8-hour dark photoperiod for another 5 days. The seedlings were transferred to test tubes and grown hydroponically in half-strength Hoagland nutrient solution (Pi-rich) or half-strength Hoagland nutrient solution without Pi (Pi-deficient) in a growth chamber under the same conditions as above for 10 days.

Plants were divided into shoots and roots, and roots were briefly washed with tap water. They were stored at −80°C until use. The SLs were extracted from the media and subjected to purification procedures as described previously (*27*).

To extract SLs from tomato plants, shoots or roots were homogenized in ethyl acetate and incubated at 4°C overnight. The filtrates were evaporated, dissolved in 1.5% ethyl acetate/*n*-hexane (v/v), loaded onto a Sep-Pak Silica 1-ml column (Waters), washed with *n*-hexane, and then eluted with 60% ethyl acetate/*n*-hexane (v/v). The eluates were evaporated, dissolved in acetonitrile, and subjected to LC-MS/MS analysis.

Cultivation condition of cowpea for RNA-seq analysis

Figure S1A shows cowpea hydroponic conditions for RNA-seq analysis. Seeds of cowpea were soaked in water and germinated at

23°C in the dark for 2 days. Then, the seedlings were transferred to test tubes and grown hydroponically in Hoagland nutrient solution (initially containing 500 μM Pi before its concentration was progressively decreased) in a growth chamber at 23°C with a 16-hour light/8-hour dark cycle for 13 days, and then the culture conditions were changed as follows: Condition (a), the culture medium was replaced with Hoagland nutrient solution containing 500 μM Pi (a1) or no Pi (a2) on day 14, and plants were harvested after growing for 24 hours. Condition (b), the culture medium was replaced with water (b1-1, b1-2) or 5 μM GR24 in water (b2-1, b2-2) on day 14, and plants were harvested after growing for 24 hours. Condition (c), after one additional day of culture in water, on day 15, the culture medium was replaced with Hoagland nutrient solution containing 500 μM Pi, and the plants were harvested after growing for 3 hours (c1), or after 12 hours, the culture medium was replaced with fresh medium, and plants were harvested after growing for another 12 hours (c2).

RNA-seq analysis and comparative coexpression analysis

Total RNA was extracted using the RNeasy Plant Mini Kit (Qiagen) from roots of cowpea (*V. unguiculata* cv. B301) cultivated under the six conditions described above. RNA quality was evaluated using a Bioanalyzer 2100 (Agilent Technologies). A 10-μg aliquot of total RNA was used to construct a cDNA library using the Illumina TruSeq Prep Kit v2 according to the manufacturer's protocol (Illumina). The resulting cDNA library was sequenced using a HiSeq1500 (Illumina) with 100–base pair (bp) paired-end reads. Total reads were assembled using CLC Genomics Workbench version 7.0 (CLC Bio) with the following parameters: Minimum contig length was 200 bp, and after adaptor sequences and low quality reads were removed, scaffolding was performed to obtain assembled contigs. For each sample, the reads were aligned to obtain reliable reads per kilobase of exon per million mapped reads (RPKM) values using CLC Genomics Workbench version 7.0 (CLC Bio).

To construct the cowpea RNA-seq dataset, we used 81,057 assembled contigs (table S2) and collected those with RPKM values of >10 under any cultivation condition, resulting in 19,417 contigs. Using this dataset, gene coexpression analysis was performed by the Confeito algorithm (*21*), and we acquired a local module including a contig sequence encoding the VuCCD8 target gene. Comprehensive functional annotations, including protein sequence similarity and GO term classification on the 131 contigs contained in the *VuCCD8* module, were performed. The contig sequences were compared with the NCBI nr (nonredundant) protein database (www.ncbi.nlm.nih.gov) using the BLASTX program with a cutoff *E* value of $<1 \times 10^{-5}$, and the maximum number of allowed hits was fixed at 10. With nr annotation, the Blast2GO program (*28*) was used to classify contigs to GO terms (data S1). The seven contigs that were annotated as CYP and were longer than 500 bp were selected as candidate genes for SL biosynthesis (table S2). The sequencing data have been submitted to the DDBJ (DNA Data Bank of Japan) Read Archive under accession no. DRA008222.

Cloning of CYP genes

A cowpea cDNA template was prepared from mRNA isolated from roots using the RNeasy Plant Mini Kit (Qiagen) and ReverTra Ace qPCR RT Mix with genomic DNA (gDNA) Remover (TOYOBO) for RT-PCR. The full-length *VuMAX1*, *VuCYP722C*, and *VuCYP728B* cDNAs were amplified using the PrimeSTAR HS DNA polymerase (TaKaRa Bio) with primer sets shown in table S3. The primers were designed using the complete CDS sequences recorded in the Phytozome database (*Vigna unguiculata* v1.0; NSF, UCR, USAID, DOE-JGI; http://phytozome.jgi.doe.gov/). A synthetic *SlCYP722C* (Solyc02g084930.3) cDNA was obtained from Eurofins Genomics. Each amplicon was cloned into the pMD19 vector (Takara Bio) according to the manufacturer's instructions. Table S4 shows gene sequences characterized in this study.

Quantitative reverse transcription polymerase chain reaction

The primer sets listed in table S5 were used to perform qRT-PCR analysis. Total RNAs were prepared from the roots of three independent lines of hydroponically cultivated cowpea and tomato plants under Pi-rich and Pi-deficient conditions, as described previously. The cDNA templates were prepared as described above and amplified using a LightCycler Nano (Roche) with GeneAce SYBR qPCR Mix α No ROX (Nippon Gene). Gene expression levels were normalized against the values obtained for the cowpea actin gene (*Vigun05g012000*), which is homologous to the previously reported reference gene *VuActin-97–like* (*Vigun04g203000*) (*29*) and is expressed at a higher level, or the tomato ubiquitin gene (*Solyc01g056940*) (*30*). Data acquisition and analysis were performed using LightCycler Nano software (Roche), and calculation of the relative gene expression levels was performed on the basis of the $2^{-\Delta\Delta CT}$ method.

In vitro enzyme activity assay

VuMAX1, *VuCYP722C*, *VuCYP728B*, and *SlCYP722C* cDNAs were ligated into a Bam HI/Sal I site of the pFASTBac1 vector (Invitrogen) to generate pFASTbac1-CYP plasmids. Then, their constructs were used to generate the corresponding recombinant Bacmid DNAs by transforming *Escherichia coli* DH10Bac competent cells (Invitrogen). Preparation of the recombinant Bacmid DNA and transfection of the *Spodoptera frugiperda 9* (*Sf9*) cells were performed according to the manufacturer's instructions (Invitrogen). CYPs were expressed in *Sf9* cells as described previously (*31*).

Microsomal fractions of insect cells expressing CYP were obtained as described previously (*32*). In vitro enzyme activities were measured by mixing the CYP-containing microsomal fraction of insect cells with purified *Arabidopsis* NADPH (reduced form of nicotinamide adenine dinucleotide phosphate)–CYP reductase (*33*). The reaction mixture consisted of 50 mM potassium phosphate (pH 7.25), 25 μl of microsomal fraction, NADPH–CYP reductase (1 U/ml), 2.5 mM NADPH, and 25 μM substrate in a total volume of 250 μl. Reactions were initiated by addition of NADPH and were performed at 30°C for 60 min. The reaction products were extracted twice using an equivalent volume of ethyl acetate. The organic phase was collected and evaporated. The residues were dissolved in acetonitrile and analyzed by LC-MS/MS.

LC-MS/MS analysis of SLs

The SLs were analyzed by LC-MS/MS using an LC-MS system (Waters) consisting of an ACQUITY Ultra Performance liquid chromatograph and an ACQUITY quadruple tandem mass spectrometer (TQ Detector). MassLynx 4.1 software (Waters) was used to perform data acquisition and analyses. The analytical conditions were carried out as described previously (*18*). Separations were performed using a two-gradient program: 50 to 100% MeOH in H_2O for 0 to 20 min (LC method I) and 50% MeOH in H_2O for 5 min and 50 to 55% MeOH in H_2O for 5 to 25 min (LC method II). MRM was used to detect the presence of SLs, and MRM transitions are summarized in table S6.

Generation of *SlCYP722C*-KO tomato plants

The *SlCYP722C*-KO tomato plants were generated by targeted genome editing with the CRISPR-Cas9 system. We used the CRISPR-Cas9 binary vector pMgP237-2A–green fluorescent protein (GFP) to express multiplex guide RNA (gRNAs) (*34*, *35*). To design the gRNA target with low off-target effects in the first exon of *SlCYP722C* (Solyc02g084930), we used the web tools sgRNA Designer (https://portals.broadinstitute.org/gpp/public/analysis-tools/sgrna-design), Cas-OT software (*36*), and CRISPR-P v2.0 (*37*). Then, we selected two target sequences, namely, target_1 and target_2 (Fig. 4A), and no potential off-target sites in *SlCYP722C* corresponding to exonic positions of other genes were found in the tomato genome (SL3.0 of Sol Genomics Network) (https://solgenomics.net/). To enhance the efficiency of gRNA transcription from the U6 promoter, one G was added to the 5′ end of target_1 and target_2. The DNA fragment composed of the gRNA and transfer RNA (tRNA) scaffolds between both target sequences was generated by PCR using pMD-gtRNA containing gRNA and tRNA scaffolds as a template and primer sets containing restriction enzyme Bsa I sites (5′-ttgggtctcgtgcagagtttgggaataccttcgtgttttagagctagaaatagca-3′ and 5′-ttgggtctccaaacacagtgtcaaaggttgttatctgcaccagccgggaatcgaa-3′). The unit containing two gRNAs-tRNA was then inserted into the Bsa I site of multiplex CRISPR-Cas9 vector pMgP237-2A-GFP using Golden Gate cloning methods to generate the CRIPR-Cas9 vector named pMgP237-SlCYP722KO1. The vector was introduced into *Agrobacterium tumefaciens* strain EHA105 by electroporation. Transgenic tomato plants (*S. lycopersicum* cv. Micro-Tom) were transformed using *A. tumefaciens* EHA105 cells harboring pMgP237-SlCYP722KO1 as reported previously (*38*). Transformants were selected using kanamycin and genomic PCR targeting a partial region of T-DNA region integrated into the genome with the primers 5′-ggcccctgggaatctgaaag-3′ and 5′-ggaagaagaaatcgatctggaaaattttgc-3′ (*34*).

Next, mutations in the targets sites of established primary T0 transformants were analyzed. Partial fragments surrounding the *SlCYP722C* target sites were amplified by PCR with 5′-agtttgggaataccttcgtggg-3′ and 5′-gttgacctagtatccgtcatctca-3′ primer sets. The PCR amplicons were visualized on 5% polyacrylamide gels (*39*). The T0 lines with extra bands, indicating the formation of heteroduplexes in the target sites, were selected to generate T1 progeny by self-pollination. gDNA was isolated from the T1 progeny obtained, and partial fragments surrounding the *SlCYP722C* target sites were amplified by PCR as described above. The PCR fragments from independent lines were cleaned using the Wizard SV Gel and PCR Clean-Up System (Promega) according to the manufacturer's instructions and cloned into pCR 4Blunt-TOPO (Invitrogen). Sanger sequencing of each of the cloned DNAs was performed using a sequencing service (Eurofins Genomics). Next, we obtained T1 lines harboring a biallelic mutation in the first exon of *SlCYP722C* (Fig. 4B). A T1 line (#2-25) produced fruits and seeds normally, and lastly, T2 progeny of nos. 2 to 25 was generated. In the T2 lines, the absence of integration of the T-DNA region into the genome was confirmed by genomic PCR with the primers used in the transformant selection. Of the T2 lines, lines with the same biallelic mutation as the T1 lines were used for further analyses.

Germination bioassay

A germination assay was conducted as reported previously (*40*). Surface-sterilized seeds were conditioned for 9 days at 30°C for *S. hermonthica*, for 5 days at 21°C for *O. crenata*, and for 5 days at 23°C for *P. aegyptiaca* on 8-mm glass-fiber filter-paper disks (approximately 50 seeds each) and then placed on distilled water–saturated filter paper. Aliquots (20 μl) of the plant hydroponic culture media were assayed by applying them to the conditioned seeds. The treated seeds were incubated at the same temperature as that used for conditioning and were microscopically examined for germination 1 day (*S. hermonthica*) or 5 days (*O. crenata* and *P. aegyptiaca*) later.

SUPPLEMENTARY MATERIALS

Supplementary material for this article is available at http://advances.sciencemag.org/cgi/content/full/5/12/eaax9067/DC1

Supplementary Text

Fig. S1. Cowpea root tissues for RNA-seq analysis.

Fig. S2. Analysis of root exudates of cowpea and tomato.

Fig. S3. In vitro enzyme assay of VuCYP722C and VuCYP728B.

Fig. S4. MRM chromatograms of root exudates and root and shoot extracts from WT and *SlCYP722C*-KO tomato plants cultivated under Pi-deficient conditions.

Table S1. Cowpea CYP genes coexpressed with *VuCCD8*.

Table S2. Summary of de novo assembly and mapping statistics.

Table S3. Primers used for gene cloning.

Table S4. CDS sequences of genes characterized in this study.

Table S5. Primers used for qRT-PCR.

Table S6. Conditions used for the detection of SLs with LC–MS/MS.

Data S1. Transcripts contained in the *VuCCD8* module generated by Confeito analysis.

Data S2. Multi-FASTA file of all contigs in transcriptome analysis of cowpea roots.

Data S3. RPKM values of all contigs in transcriptome analysis of cowpea roots.

View/request a protocol for this paper from *Bio-protocol*.

REFERENCES AND NOTES

1. V. Gomez-Roldan, S. Fermas, P. B. Brewer, V. Puech-Pagès, E. A. Dun, J.-P. Pillot, F. Letisse, R. Matusova, S. Danoun, J.-C. Portais, H. Bouwmeester, G. Bécard, C. A. Beveridge, C. Rameau, S. F. Rochange, Strigolactone inhibition of shoot branching. *Nature* **455**, 189–194 (2008).
2. M. Umehara, A. Hanada, S. Yoshida, K. Akiyama, T. Arite, N. Takeda-Kamiya, H. Magome, Y. Kamiya, K. Shirasu, K. Yoneyama, J. Kyozuka, S. Yamaguchi, Inhibition of shoot branching by new terpenoid plant hormones. *Nature* **455**, 195–200 (2008).
3. B. Zwanenburg, D. Blanco-Ania, Strigolactones: New plant hormones in the spotlight. *J. Exp. Bot.* **69**, 2205–2218 (2018).
4. C. E. Cook, L. P. Whichard, B. Turner, M. E. Wall, G. H. Egley, Germination of witchweed (*striga lutea* lour.): Isolation and properties of a potent stimulant. *Science* **154**, 1189–1190 (1966).
5. H. Samejima, A. G. Babiker, A. Mustafa, Y. Sugimoto, Identification of *Striga hermonthica*-resistant upland rice varieties in Sudan and their resistance phenotypes. *Front. Plant Sci.* **7**, 634 (2016).
6. K. Yoneyama, X. Xie, D. Kusumoto, H. Sekimoto, Y. Sugimoto, Y. Takeuchi, K. Yoneyama, Nitrogen deficiency as well as phosphorus deficiency in sorghum promotes the production and exudation of 5-deoxystrigol, the host recognition signal for arbuscular mycorrhizal fungi and root parasites. *Planta* **227**, 125–132 (2007).
7. K. Ueno, T. Furumoto, S. Umeda, M. Mizutani, H. Takikawa, R. Batchvarova, Y. Sugimoto, Heliolactone, a non-sesquiterpene lactone germination stimulant for root parasitic weeds from sunflower. *Phytochemistry* **108**, 122–128 (2014).
8. H. Il Kim, T. Kisugi, P. Khetkam, X. Xie, K. Yoneyama, K. Uchida, T. Yokota, T. Nomura, C. S. P. McErlean, K. Yoneyama, Avenaol, a germination stimulant for root parasitic plants from *Avena strigosa*. *Phytochemistry* **103**, 85–88 (2014).
9. T. V. Charnikhova, K. Gaus, A. Lumbroso, M. Sanders, J.-P. Vincken, A. De Mesmaeker, C. P. Ruyter-Spira, C. Screpanti, H. J. Bouwmeester, Zealactones. Novel natural strigolactones from maize. *Phytochemistry* **137**, 123–131 (2017).
10. X. Xie, N. Mori, K. Yoneyama, T. Nomura, K. Uchida, K. Yoneyama, K. Akiyama, Lotuslactone, a non-canonical strigolactone from *Lotus japonicus*. *Phytochemistry* **157**, 200–205 (2019).
11. K. Yoneyama, X. Xie, K. Yoneyama, T. Kisugi, T. Nomura, Y. Nakatani, K. Akiyama, C. S. P. McErlean, Which are the major players, canonical or non-canonical strigolactones? *J. Exp. Bot.* **69**, 2231–2239 (2018).
12. A. Alder, M. Jamil, M. Marzorati, M. Bruno, M. Vermathen, P. Bigler, S. Ghisla, H. Bouwmeester, P. Beyer, S. Al-Babili, The path from β-carotene to carlactone, a strigolactone-like plant hormone. *Science* **335**, 1348–1351 (2012).
13. Y. Seto, A. Sado, K. Asami, A. Hanada, M. Umehara, K. Akiyama, S. Yamaguchi, Carlactone is an endogenous biosynthetic precursor for strigolactones. *Proc. Natl. Acad. Sci. U.S.A.* **111**, 1640–1645 (2014).

14. S. Abe, A. Sado, K. Tanaka, T. Kisugi, K. Asami, S. Ota, H. I. Kim, K. Yoneyama, X. Xie, T. Ohnishi, Y. Seto, S. Yamaguchi, K. Akiyama, K. Yoneyama, T. Nomura, Carlactone is converted to carlactonoic acid by MAX1 in *Arabidopsis* and its methyl ester can directly interact with AtD14 in vitro. *Proc. Natl. Acad. Sci. U.S.A.* **111**, 18084–18089 (2014).
15. K. Yoneyama, N. Mori, T. Sato, A. Yoda, X. Xie, M. Okamoto, M. Iwanaga, T. Ohnishi, H. Nishiwaki, T. Asami, T. Yokota, K. Akiyama, K. Yoneyama, T. Nomura, Conversion of carlactone to carlactonoic acid is a conserved function of MAX1 homologs in strigolactone biosynthesis. *New Phytol.* **218**, 1522–1533 (2018).
16. Y. Zhang, X. Cheng, Y. Wang, C. Díez-Simón, K. Flokova, A. Bimbo, H. J. Bouwmeester, C. Ruyter-Spira, The tomato MAX1 homolog, SlMAX1, is involved in the biosynthesis of tomato strigolactones from carlactone. *New Phytol.* **219**, 297–309 (2018).
17. Y. Zhang, A. D. J. van Dijk, A. Scaffidi, G. R. Flematti, M. Hofmann, T. Charnikhova, F. Verstappen, J. Hepworth, S. van der Krol, O. Leyser, S. M. Smith, B. Zwanenburg, S. Al-Babili, C. Ruyter-Spira, H. J. Bouwmeester, Rice cytochrome P450 MAX1 homologs catalyze distinct steps in strigolactone biosynthesis. *Nat. Chem. Biol.* **10**, 1028–1033 (2014).
18. M. Iseki, K. Shida, K. Kuwabara, T. Wakabayashi, M. Mizutani, H. Takikawa, Y. Sugimoto, Evidence for species-dependent biosynthetic pathways for converting carlactone to strigolactones in plants. *J. Exp. Bot.* **69**, 2305–2318 (2018).
19. K. Ueno, H. Nakashima, M. Mizutani, H. Takikawa, Y. Sugimoto, Bioconversion of 5-deoxystrigol stereoisomers to monohydroxylated strigolactones by plants. *J. Pestic. Sci.* **43**, 198–206 (2018).
20. K. Mashiguchi, E. Sasaki, Y. Shimada, M. Nagae, K. Ueno, T. Nakano, K. Yoneyama, Y. Suzuki, T. Asami, Feedback-regulation of strigolactone biosynthetic genes and strigolactone-regulated genes in Arabidopsis. *Biosci. Biotechnol. Biochem.* **73**, 2460–2465 (2009).
21. Y. Ogata, N. Sakurai, H. Suzuki, K. Aoki, K. Saito, D. Shibata, The prediction of local modular structures in a co-expression network based on gene expression datasets. *Genome Inform.* **23**, 117–127 (2009).
22. D. Nelson, D. Werck-Reichhart, A P450-centric view of plant evolution. *Plant J.* **66**, 194–211 (2011).
23. S. Hasegawa, T. Tsutsumi, S. Fukushima, Y. Okabe, J. Saito, M. Katayama, M. Shindo, Y. Yamada, K. Shimomura, K. Yoneyama, K. Akiyama, K. Aoki, T. Ariizumi, H. Ezura, S. Yamaguchi, M. Umehara, Low infection of *Phelipanche aegyptiaca* in Micro-Tom mutants deficient in CAROTENOID CLEAVAGE DIOXYGENASE 8. *Int. J. Mol. Sci.* **19**, 2645 (2018).
24. C. Parker, Observations on the current status of Orobanche and striga problems worldwide. *Pest Manag. Sci.* **65**, 453–459 (2009).
25. N. Mori, K. Nishiuma, T. Sugiyama, H. Hayashi, K. Akiyama, Carlactone-type strigolactones and their synthetic analogues as inducers of hyphal branching in arbuscular mycorrhizal fungi. *Phytochemistry* **130**, 90–98 (2016).
26. K. Ueno, S. Nomura, S. Muranaka, M. Mizutani, H. Takikawa, Y. Sugimoto, *Ent*-2′-*epi*-orobanchol and its acetate, as germination stimulants for *Striga gesnerioides* seeds isolated from cowpea and red clover. *J. Agric. Food Chem.* **59**, 10485–10490 (2011).
27. N. Motonami, K. Ueno, H. Nakashima, S. Nomura, M. Mizutani, H. Takikawa, Y. Sugimoto, The bioconversion of 5-deoxystrigol to sorgomol by the sorghum, *Sorghum bicolor* (L.) Moench. *Phytochemistry* **93**, 41–48 (2013).
28. A. Conesa, S. Götz, J. M. García-Gómez, J. Terol, M. Talón, M. Robles, Blast2GO: A universal tool for annotation, visualization and analysis in functional genomics research. *Bioinformatics* **21**, 3674–3676 (2005).
29. L. L. B. Amorim, J. R. C. Ferreira-Neto, J. P. Bezerra-Neto, V. Pandolfi, F. T. de Araújo, M. K. da Silva Matos, M. G. Santos, E. A. Kido, A. M. Benko-Iseppon, Cowpea and abiotic stresses: Identification of reference genes for transcriptional profiling by qPCR. *Plant Methods* **14**, 88 (2018).
30. P. A. Ofori, A. Mizuno, M. Suzuki, E. Martinoia, S. Reuscher, K. Aoki, D. Shibata, S. Otagaki, S. Matsumoto, K. Shiratake, Genome-wide analysis of ATP binding cassette (ABC) transporters in tomato. *PLOS ONE* **13**, e0200854 (2018).
31. S. Saito, N. Hirai, C. Matsumoto, H. Ohigashi, D. Ohta, K. Sakata, M. Mizutani, Arabidopsis CYP707As encode (+)-abscisic acid 8′-hydroxylase, a key enzyme in the oxidative catabolism of abscisic acid. *Plant Physiol.* **134**, 1439–1449 (2004).
32. T. Ohnishi, A.-M. Szatmari, B. Watanabe, S. Fujita, S. Bancos, C. Koncz, M. Lafos, K. Shibata, T. Yokota, K. Sakata, M. Szekeres, M. Mizutani, C-23 hydroxylation by Arabidopsis CYP90C1 and CYP90D1 reveals a novel shortcut in brassinosteroid biosynthesis. *Plant Cell* **18**, 3275–3288 (2006).
33. M. Mizutani, D. Ohta, Two isoforms of NADPH:Cytochrome P450 reductase in Arabidopsis thaliana. Gene structure, heterologous expression in insect cells, and differential regulation. *Plant Physiol.* **116**, 357–367 (1998).
34. M. Nakayasu, R. Akiyama, H. J. Lee, K. Osakabe, Y. Osakabe, B. Watanabe, Y. Sugimoto, N. Umemoto, K. Saito, T. Muranaka, M. Mizutani, Generation of α-solanine-free hairy roots of potato by CRISPR/Cas9 mediated genome editing of the *St16DOX* gene. *Plant Physiol. Biochem.* **131**, 70–77 (2018).
35. R. Hashimoto, R. Ueta, C. Abe, Y. Osakabe, K. Osakabe, Efficient multiplex genome editing induces precise, and self-ligated type mutations in tomato plants. *Front. Plant Sci.* **9**, 916 (2018).
36. A. Xiao, Z. Cheng, L. Kong, Z. Zhu, S. Lin, G. Gao, B. Zhang, CasOT: A genome-wide Cas9/gRNA off-target searching tool. *Bioinformatics* **30**, 1180–1182 (2014).
37. H. Liu, Y. Ding, Y. Zhou, W. Jin, K. Xie, L.-L. Chen, CRISPR-P 2.0: An improved CRISPR-Cas9 tool for genome editing in plants. *Mol. Plant* **10**, 530–532 (2017).
38. H.-J. Sun, S. Uchii, S. Watanabe, H. Ezura, A highly efficient transformation protocol for Micro-Tom, a model cultivar for tomato functional genomics. *Plant Cell Physiol.* **47**, 426–431 (2006).
39. S. Ota, Y. Hisano, M. Muraki, K. Hoshijima, T. J. Dahlem, D. J. Grunwald, Y. Okada, A. Kawahara, Efficient identification of TALEN-mediated genome modifications using heteroduplex mobility assays. *Genes Cells* **18**, 450–458 (2013).
40. Y. Sugimoto, A. M. Ali, S. Yabuta, H. Kinoshita, S. Inanaga, A. Itai, Germination strategy of *Striga hermonthica* involves regulation of ethylene biosynthesis. *Physiol. Plant.* **119**, 137–145 (2003).

Acknowledgments: The authors thank A. Gabar Babiker (National Center for Research, Sudan) for providing seeds of root parasitic weeds and the University of Tsukuba, Gene Research Center (Japan) and M. Umehara (Toyo University, Japan) for providing seeds of tomato WT and Slccd8 mutant through National Bio-Resource Project of the Japan Agency for Medical Research and Development. **Funding:** This work was supported, in part, by JST/JICA SATREPS (JPMJSA1607 to Y.S.) and JSPS KAKENHI (25292065 and 19H02897 to Y.S.). **Author contributions:** T.W., M.M., and Y.S. planned and designed the experiment. T.W., M.H., and A.M. performed protein expression and enzyme assay. K.U. and H.S. performed RNA-seq, and T.W. and M.M analyzed the data. R.A., K.O., and Y.O. designed and constructed CRISPR-Cas9 vector pMgP237-SlCYP722KO1. M.H. performed generation of KO tomato plants. H.T. performed chemical synthesis of SLs. T.W., M.H., and A.M. performed LC-MS/MS analysis of root exudates. T.W. and Y.S. wrote the paper with input from all authors. **Competing interests:** The authors declare that they have no competing interest. **Data and materials availability:** The RNA-seq data are deposited in the DDBJ Read Archive under accession no. DRA008222. Multi-FASTA file and RPKM values of all contigs in the RNA-seq analysis are presented in data S2 and S3, respectively. All data needed to evaluate the conclusions in the paper are present in the paper and/or the Supplementary Materials. Additional data related to this paper may be requested from the authors.

Submitted 3 May 2019
Accepted 1 November 2019
Published 18 December 2019
10.1126/sciadv.aax9067

Citation: T. Wakabayashi, M. Hamana, A. Mori, R. Akiyama, K. Ueno, K. Osakabe, Y. Osakabe, H. Suzuki, H. Takikawa, M. Mizutani, Y. Sugimoto, Direct conversion of carlactonoic acid to orobanchol by cytochrome P450 CYP722C in strigolactone biosynthesis. *Sci. Adv.* **5**, eaax9067 (2019).

ScienceAdvances

Direct conversion of carlactonoic acid to orobanchol by cytochrome P450 CYP722C in strigolactone biosynthesis

Takatoshi Wakabayashi, Misaki Hamana, Ayami Mori, Ryota Akiyama, Kotomi Ueno, Keishi Osakabe, Yuriko Osakabe, Hideyuki Suzuki, Hirosato Takikawa, Masaharu Mizutani and Yukihiro Sugimoto

Sci Adv **5** (12), eaax9067.
DOI: 10.1126/sciadv.aax9067